Journal of Photochemistry & Photobiology, B: Biology 176 (2017) 25–35

Contents lists available at ScienceDirect

Journal of Photochemistry & Photobiology, B: Biology

journal homepage: www.elsevier.com/locate/jphotobiol

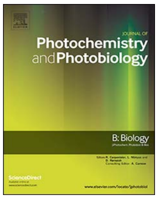

# Effect of porphyrin on photocatalytic activity of $TiO_2$ nanoparticles toward Rhodamine B photodegradation

M.A. Ahmed, Z.M. Abou-Gamra*, H.A.A. Medien, M.A. Hamza

*Chemistry Department, Faculty of Science, Ain-Shams University, Abbassia, Cairo, Egypt*

ARTICLE INFO

*Keywords:*
Porphyrin-$TiO_2$
Photosensitization
Photodegradation
Rhodamine B

ABSTRACT

As known, porphyrins have central role in photosynthesis, biological oxidation and reduction and oxygen transport beside to their intensive color which qualify them to be good photosensitizers. Herein, tetra (4-carboxyphenyl) porphyrin (TCPP) was prepared by a simple one-pot synthesis to use as a visible antenna for $TiO_2$ nanoparticles that were prepared via a simple template-free sol-gel method. Various loading percentages of TCPP (0.05–1%) were incorporated on the surface of $TiO_2$ as photosensitizer for photocatalytic degradation of Rhodamine B (Rh B) dye as a primary cationic pollutant model. Among them, 0.1% TCPP-$TiO_2$ was the most reactive sample. It was found that the photoactivity of 0.1% TCPP-$TiO_2$ sample (0.5 g/L) was approximately 1.5 times greater than that of pure $TiO_2$ (0.5 g/L) toward the degradation of Rh B ($1 \times 10^{-5}$ M) under UV-A irradiation. Transient fluorescence decay measurements showed that the life time of $TiO_2$ excited state has doubled after anchoring TCPP, thus the probability of electron-hole recombination has decreased. The samples were characterized by XRD, HR-TEM, DRS and $N_2$ adsorption-desorption isotherms. The XRD patterns confirmed the successful preparation of $TiO_2$ nanoparticles with average crystalline size of 25.7 nm. Also, XRD patterns suggested the presence of mixed phase $TiO_2$ nanoparticles of 77% anatase and 23% rutile. DRS showed that the characteristic peaks of TCPP covered the whole visible range 400–700 nm. HR-TEM images showed the spheroids shape of $TiO_2$ nanoparticles and confirmed the presence of anatase and rutile phases as suggested from XRD data. The different parameters affecting the photodegradation of Rh B dye such as catalyst dose, dye concentration and pH were studied to obtain the optimum conditions. Almost complete degradation of Rh B was obtained which confirmed by HPLC and TOC measurements. The effect of scavengers was studied to indicate the most active species. TCPP-$TiO_2$ gave a good response toward the photodegradation of Rh B under visible irradiation. Finally, the mechanism of photocatalytic degradation process was suggested.

## 1. Introduction

Our world extremely suffers from pollution due to urgent need to industry such as textile, paper printing, Leather and drugs. Textile processes are discharging large quantities of dyes in the environment. These dyes can be considered one of the most common sources of water pollution because they constitute a group of hazardous organic compounds and 700,000 t of them are produced in the world annually. About 15% of the total world production of dyes is released in textile effluents during textile dyeing [1,2]. The discharge of highly colored waste can affect the aquatic organisms either directly due to the toxicity of most of dyes or indirectly by preventing their biological processes by impeding the light penetration [3]. Rhodamine B dye was detected in wastewater as reported earlier [4,5] which causes irritation of eyes, skin, respiratory and gastrointestinal tracts [6]. Hence, there is an urgent necessity to remove these hazardous pollutants from water.

Various traditional methods such as chemical precipitation, solvent extraction, reverse osmosis, adsorption, ion exchange and filtration were employed in water treatment but they are non-destructive techniques as they cannot completely degrade the pollutants but they only transfer them from water into another medium [7]. Advanced oxidation processes (AOPs) such as $H_2O_2$-UV [8] and Fenton processes [9] which depend on production of highly reactive oxidizing species were succeeded in waste water treatment. In the last decades, semiconductor-assisted photocatalysis was intensively studied as it is considered as 'green' method for wastewater treatment [10–26].

Titanium oxide ($TiO_2$) is one of the most important photocatalysts due to its non-toxicity, availability, stability and excellent photocatalytic performance. Unfortunately, it has two major disadvantages: its rapid electron-hole recombination rate causing decreasing of its photocatalytic efficiency and its large band gap energy (3.2 eV for pure anatase) causing excluding its activity only under UV irradiation which

---

* Corresponding author.
*E-mail address:* zanibabougamra@yahoo.com (Z.M. Abou-Gamra).

http://dx.doi.org/10.1016/j.jphotobiol.2017.09.016
Received 4 June 2017; Received in revised form 29 August 2017; Accepted 15 September 2017

represents only 2–3% of whole solar-light spectrum [10–24]. Several techniques are used to overcome these disadvantages such as metal doping [10,17,21,23,24], non-metal doping [11,13,18,20], co-doping [14,22] and dye sensitization using curcumin [27], phthalocyanine [28], porphyrins and metal porphyrin [29–46].

Porphyrins with their intensive colors are suggested to shift the photocatalytic response of $TiO_2$ to the visible region and prevents the electron–hole recombination [38,39,43]. A. Kathiravan and R. Renganathan [36] studied the effect of anchoring group on the photosensitization of $TiO_2$ nanoparticles by four different porphyrins among which TCPP was the most efficient photosensitizer. S. Murphy et al. [33] studied the adsorption of commercial TCPP on P25 (Degussa) by two methods where the first was performed in methanol at room temperature while the second was performed in dimethylformamide (DMF) at reflux. They deduced that the formed composites from the two methods have the same physical, chemical characteristics and the photocatalytic activity against some pharmaceuticals. H. Wang et al. [29] studied the photosensitization of commercial P25 with synthesized TCPP and tested its photocatalytic activity toward the degradation of methylene blue dye under visible light. They found that TCPP-P25 catalyst has weak photoactivity in comparison to its relatively high adsorption.

This study is concerned with the preparation of TCPP, $TiO_2$ and different percent of TCPP (0.05–1%) over $TiO_2$ nanoparticles. Photocatalytic activities of the as prepared samples were examined toward the degradation of Rh B. Among them, 0.1%TCPP-$TiO_2$ was the most active catalyst.

Pure $TiO_2$ and 0.1% TCPP-$TiO_2$ were characterized by XRD, DRS, HR-TEM and $N_2$ adsorption-desorption isotherms. The different parameters affecting the photodegradation of Rh B dye such as catalyst dose, dye concentration and pH were studied. HPLC and TOC measurements were utilized to confirm the mineralization of the Rh B. Also, the photocatalytic activity of TCPP-$TiO_2$ under visible irradiation was investigated. Finally, the effect of scavengers was studied to indicate the active species and the mechanism of the photodegradation of Rh B using TCPP-$TiO_2$ was suggested.

## 2. Experimental

### 2.1. Materials

Pyrrole, 4-carboxybenzaldehyde, propionic acid, methanol and Rhodamine B were purchased from Merck (Darmstadt, Germany). Titanium tetra-isopropoxide (TTIP) 97%, *p*-benzoquinone 98.5% and methyl viologen were purchased from sigma-Aldrich (St. Louis, MO, USA). Acetonitrile and water of HPLC grade were purchased from Fisher Scientific Company (Waltham, MA, USA). All other chemicals were of pure grade and used without further purification. All solutions were prepared using distilled water. The pH was adjusted by HCl and NaOH solutions.

### 2.2. Preparation of TCPP

TCPP was prepared via a simple one-pot synthesis (Scheme 1) as previously described [47]. It was prepared directly by refluxing propionic acid solution in presence of 0.24 M of both 4-carboxybenzaldhye and pyrrole for 2 h. Purple crystals were obtained by cooling mixture and further purified from methanol-chloroform solution.

### 2.3. Preparation of $TiO_2$ Nanoparticles

$TiO_2$ nanoparticles were prepared via a simple template-free sol-gel method. Firstly, 25 mL of TTIP were dissolved in 250 mL of isopropyl alcohol and 75 mL of ethylene glycol. The solution was stirred using magnetic stirrer at 700 rpm for 1 h. An appropriate amount of distilled water was added to the above solution dropwise and the white colloid particles increased gradually as the hydrolysis reaction proceeds until a milky-like gel was formed with continuous stirring for 2 h. After 2 days of aging, the gel was filtered and washed by distilled water and isopropanol. Finally, the gel was dried at 100 °C for 20 h and calcined at 550 °C for 4 h.

### 2.4. Preparation of TCPP-$TiO_2$ Nanoparticles

TCPP-$TiO_2$ nanoparticles were prepared using wet impregnation method. Various loadings (0.05–1%) of TCPP were dissolved in methanol and then $TiO_2$ nanoparticles were added on the solution to obtain different percentages of TCPP on $TiO_2$. The solutions were stirred for 8 h and left for 2 days for aging. The solutions were filtered and washed by methanol. Finally, the solids were collected and dried at 100 °C for 2 h. The prepared samples were denoted as $x$% TCPP-$TiO_2$ where $x$ represents the weight percent of TCPP with respect to $TiO_2$.

### 2.5. Physicochemical Characterization

The structure of TCPP was confirmed by UV–Visible and NMR spectra. TCPP was dissolved in methanol to detect its UV–Vis spectrum that measured on T92 + UV–Vis spectrophotometer (PG instruments, Lutterworth, UK). $^1H$ NMR and $^{13}C$ NMR spectra were recorded on Mercury 400 MHz spectrometer (Oxford, Abingdon, UK) equipped with Varian 5 MM probe. DMSO-$d_6$ was used as solvents for $^1H$ NMR and $^{13}C$ NMR analyses and chemical shifts have been expressed in parts per million (ppm).

X-ray diffraction patterns were carried out by X, PERT–PRO–PANalytical X-ray diffractometer (PANalytical, Almelo, Netherlands) with CuKα (λ = 1.5406 Å) radiation in the 2θ range from 4° to 80°. The scanning mode is continuous with step size of 0.02° and scan step time of 0.5 s. The average crystallite sizes are calculated from the diffraction of peak broadening using the Scherrer equation, Eq. (1):

$$D = \frac{k\lambda}{\beta\cos\theta} \tag{1}$$

where D is the average crystallite size (nm), k is the shape factor of the particles (k = 0.9), λ is the wavelength of the X-rays (λ = 0.115406 nm), β and θ are the full width at half maximum of the peak (FWHM) and the diffraction angle (in radians), respectively.

The absorption profiles of the prepared catalysts were elucidated from diffuse reflectance spectra (DRS) that were measured by UV-2600 UV–Vis spectrophotometer (Shimadzu, Kyoto, Japan) over the range of 200–800 nm where $BaSO_4$ was used as a reference material. The band gap energy of semiconductors was calculated by Eq. (2):

$$E = h\nu = \frac{hc}{\lambda} = \frac{1240.8}{\lambda} \tag{2}$$

where E is the light energy (eV), h is Planck's constant ($6.626 \times 10^{-34}$ J·s), $\nu$ is the light frequency, c is the light velocity ($3 \times 10^8\ ms^{-1}$) and λ is the wavelength (nm).

Transient fluorescence decay and excited state lifetime measurements were performed on Easylife™ (OBB corporation, New Jersey, USA) using PTI nanosecond pulsed LED (340 nm) as an excitation light source.

Tecnai G20 high resolution transmission electron microscope (HR-TEM, FEI, Eindhoven, Netherlands) was used for imaging, crystal structure revelation and qualitative and semi-quantitative elemental analysis. TEM imaging and analysis (TIA) software were used to spectrum acquisition and analysis of energy dispersive X-ray (EDX) peaks.

$N_2$ adsorption–desorption isotherms at 77 K were measured using Nova 3200 system (Quantachrome instruments, Florida, USA). The Brunauer–Emmett–Teller (BET) method was utilized to calculate the specific surface areas (BET) from the adsorption data in a relative pressure range from 0.05 to 0.35. The Barrett–Joyner–Halenda (BJH) model [48,49] was used to estimate the average pore size from the